Comparison of turbulence models in predicting the flow around a surface mounted cube

John Doe

Abstract

Numerical experiments of a flow around a surface mounted cube in a fully turbulent channel flow was carried out with the open source CFD-tool OpenFOAM® 1.9x. Different turbulence models have been tested and the obtained results have been compared with experimental observations by Martinzzi and Tropea (1993), investigating the accuracy of each turbulence model in predicting the mean streamwise velocity profile and the surface pressure coefficient. The numerical computational domain, boundary and initial conditions have been chosen in order to replicate the experimental set-up. The results show an agreement with similar works present in literature highlighting the better performance of the k-epsilon models family in forecast the experimental data.

1 Introduction

The study of flows around surface mounted obstacles is fundamental to understand the basics of building aerodynamics, with connection to other fluid mechanics fields, such as car and train aerodynamics, heat transfer of electronic elements (Becker et al. 2002), pollutant dispersion in urban environment etc., resulting in a challenging case for the Computational Fluid Dynamics. In literature are present experimental studies of this kind of flow. Some studies were done by Castro and Robins (1977), Hunt et al. (1978), Schofield and Logan (1990), Larousse et al. (1993) and Hussein and Martinuzzi (1996). The best documented experimental work concerning the flow around a surface mounted is from Martinuzzi and Tropea (1993). On the other hand, in literature are present also a considerable number of works related to the investigation of flow around bluff body exploiting the CFD, focusing on selecting the appropriate grid configuration and the corresponding turbulence model using the wall y^+ as guidance (Ariff et al., 2009). Breuer et al. (1996), reported a comparative study between LES (Large Eddy Simulation) and RANS (Raynolds Averaged Navier-Stokes) equations, comparing the results with measurements; Lindmeier et al. (2010) tested the performance of different turbulence models for the calculation of the flow around three dimensional model buildings, arrays and a three dimensional hill, with the open source CFD-tool OpenFOAM® 1.6x and Fluent® 12. Other numerical studies on this kind of topic has been performed: Gao and

Chow (2005) performed RANS simulations, while Krajnovic and Davidson (2002) and Yang and Ferzieger (1993) performed LES simulations showing a good agreement of the computed velocity profile with experimental data.

The goal of this work is to present results of channel flow around a cube using the open source CFD-tool OpenFoam® 1.9x; numerical experiments has been performed by RANS simulations employing different turbulence models, such as standard k-epsilon model, k-omega SST model and Realizable k-epsilon model. Comparison, also has been made with a validation case supplied by OpenFoam®, using the Spalart-Allmaras Improved Delayed Detached Eddy Simulation (SA-IDDES); its reported results are obtained without change the settings provided by OpenFoam® 1.9x. The study will focus not only in reproducing the mean velocity profile upwind and downwind of the cube, but also in compute the surface pressure coefficient (C_p), compering the obtained results with experimental data from Martinuzzi and Tropea (1993).

The paper is structured as follow: in Section 2 will be presented the numerical set-up and the description of the investigated cases; in Section 3 the results of the comparison between the computed and experimental data are reported; finally, Section 4 draws the conclusion.

2. Numerical set-up

The numerical set-up of the performed numerical experiments and the computational domain shown in Fig. 1, replicates the experimental set-up of Martinuzzi and Tropea (1993). No-slip conditions were applied on the bottom, top and all cube faces, whereas the side walls were defined as slip boundary conditions. A fully developed turbulent flow was set at the inlet, where the velocity profile replicates the experiment, with a Reynolds number based on the height of the channel, Re_h = 10^4, where $Re_h=Uh/v$, with U being the characteristic flow velocity, h the height of the channel and v the cinematic viscosity.

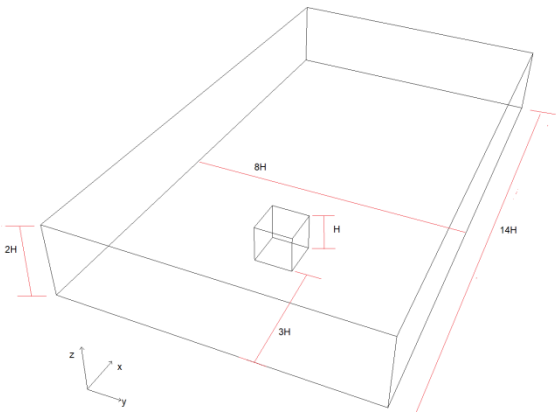

Figure 1. Computational geometry of the numerical simulations.

The same geometry has been used for all numerical experiments, where the number of cells varies in function of the turbulence model employed. It has been used hexahedral mesh with non-orthogonality 0 and maximum skewness *O*(-13). For the k-omega SST model a finer mesh was adopted in order to have an accurate wall resolved treatment with an overall y^+ mean value of 4. For the k-epsilon and Realizable k-epsilon model a wall function approach has been chosen, where the y^+ value is 38 and 32, respectively. All the analysed cases have a refinement of the mesh around the cube area useful, to improve the solution in that area of interest, where the typical horse-shoe vortex occurs. Fig. 2 shows an example of employed mesh.

(a)

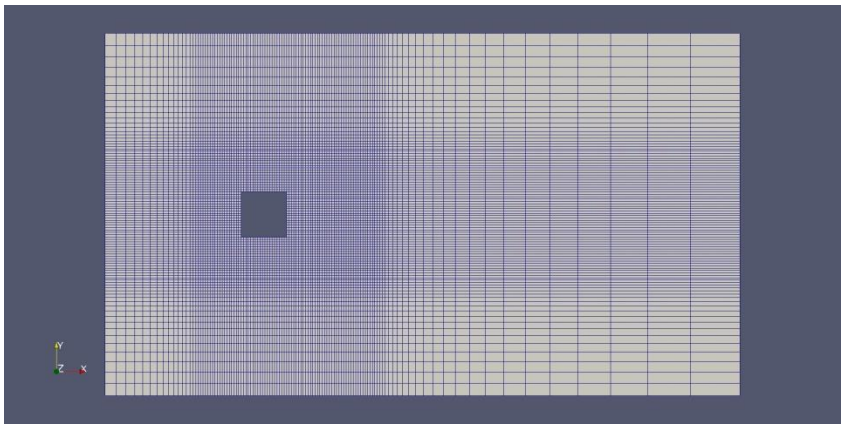

(b)

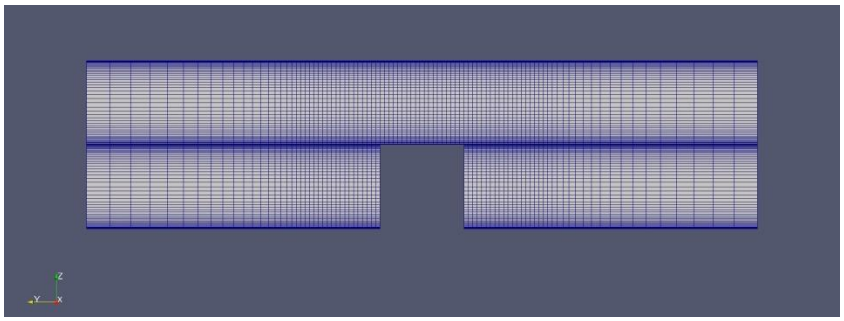

(c)

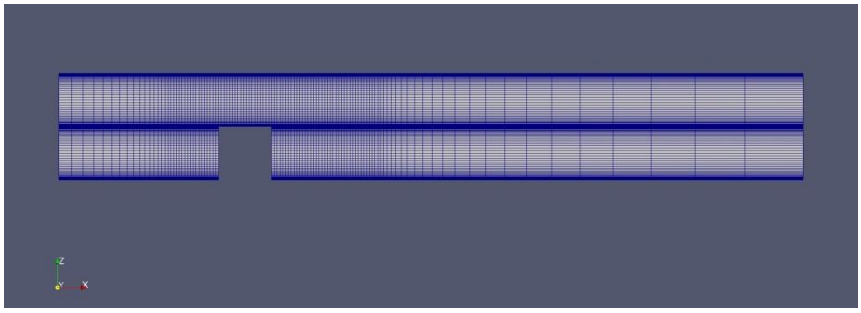

Figure 2. (a) top view of the computational grid; (b) front view; (c) side view. The grid showed here, as example, was employed for the k-omega SST case.

The details on boundary/initial conditions used for each numerical experiment are reported from Table 1 to Table 4.

K-epsilon

	Inlet	Outlet	Sides	Bottom	Top	Cube
U	MappedFixedValue	zeroGradient	Slip	NoSlip	NoSlip	NoSlip
P	zeroGradient	fixedValue	Slip	zeroGradient	zeroGradient	zeroGradient
k	MappedFixedValue	zeroGradient	Slip	kqRWallFunction	kqRWallFunction	kqRWallFunction
epsilon	MappedFixedValue	zeroGradient	Slip	epsilonWallFunction	epsilonWallFunction	epsilonWallFunction
nut	calculated	calculated	Slip	nutUWallFunction	nutUWallFunction	nutUWallFunction

Table 1. Boundary condition for the k-epsilon case.

K-omega SST

	Inlet	Outlet	Sides	Bottom	Top	Cube
U	MappedFixedValue	zeroGradient	Slip	NoSlip	NoSlip	NoSlip
P	zeroGradient	fixedValue	Slip	zeroGradient	zeroGradient	zeroGradient
k	MappedFixedValue	zeroGradient	Slip	kqRWallFunction	kqRWallFunction	kqRWallFunction
omega	MappedFixedValue	zeroGradient	Slip	omegaWallFunction	omegaWallFunction	omegaWallFunction
nut	calculated	calculated	Slip	nutUSpaldingWallFunction	nutUSpaldingWallFunction	nutUSpaldingWallFunction

Table 2. Boundary condition for the k-omega SST case.

Realizable k-epsilon

	Inlet	Outlet	Sides	Bottom	Top	Cube
U	MappedFixedValue	zeroGradient	Slip	NoSlip	NoSlip	NoSlip
P	zeroGradient	fixedValue	Slip	zeroGradient	zeroGradient	zeroGradient
k	MappedFixedValue	zeroGradient	Slip	kqRWallFunction	kqRWallFunction	kqRWallFunction
epsilon	MappedFixedValue	zeroGradient	Slip	epsilonWallFunction	epsilonWallFunction	epsilonWallFunction
nut	calculated	calculated	Slip	nutUWallFunction	nutUWallFunction	nutUWallFunction

Table 3. Boundary condition for the Realizable k-epsilon case.

SA-IDDES

	Inlet	Outlet	Sides	Bottom	Top	Cube
U	turbulentDFSEMInlet	zeroGradient	Slip	NoSlip	NoSlip	NoSlip
P	zeroGradient	fixedValue	Slip	zeroGradient	zeroGradient	zeroGradient
k	MappedFixedValue	zeroGradient	Slip	kqRWallFunction	kqRWallFunction	kqRWallFunction
nuTilda	MappedFixedValue	zeroGradient	Slip	fixedValue	fixedValue	fixedValue
nut	calculated	calculated	Slip	nutUSpaldingWallFunction	nutUSpaldingWallFunction	nutUSpaldingWallFunction

Table 4. Boundary condition for the Spalart-Allmaras Improved Delayed Detached Eddy Simulation case.

Here the settings are provided by OpenFoam® 1.9x.

In order to ensure the accuracy of the solution, a proper discretized scheme has been selected for each investigated case inside the numerical model. The discretization schemes used and the number of cells employed for the simulations are listed in Table 5.

Model	Time derivative	Divergence	Gradient	Laplacian	N. of cells
k-epsilon	steadyState	Gauss linearUpwind	Gauss linear	Gauss linear corrected	1359319
k-omega SST	steadyState	Gauss linearUpwind	cellLimited Gauss linear	Gauss linear corrected	5210750
Real. K-epsilon	steadyState	Gauss linearUpwind	Gauss linear	Gauss linear corrected	1422807
SA-IDDES	backward	Gauss DEShybrid	leastSquares	Gauss linear orthogonal	1216000

Table 5. Discretization schemes and number of cells used for the investigated cases. The settings for SA_IDDES are provided by OpenFoam® 1.9x.

3. Results

A series of time-averaged resolved velocities and pressure coefficient (C_p) are computed and compared with the experimental data of Martinuzzi and Tropea (1993). The results are evaluated in different positions, upwind, on the roof of the cube, and downstream of the front edge of the cube, which is the area where the effect of the selected model is expected to be more pronounced.

3.1 Mean velocity profile

In Fig. 3 are reported the mean velocity profiles for different positions in the channel flow obtained using RANS simulations employing three different turbulence models, such as standard k-epsilon, k-omega SST, Realizable k-epsilon, and Spalart-Allmaras IDDES. Those results are superimposed to experimental data by Martinuzzi and Tropea (1993).

(a) **(b)**

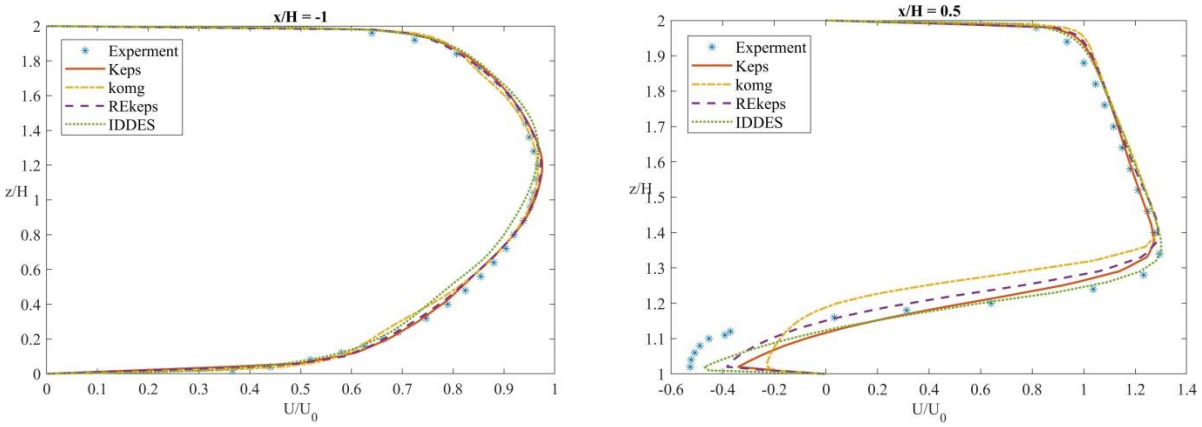

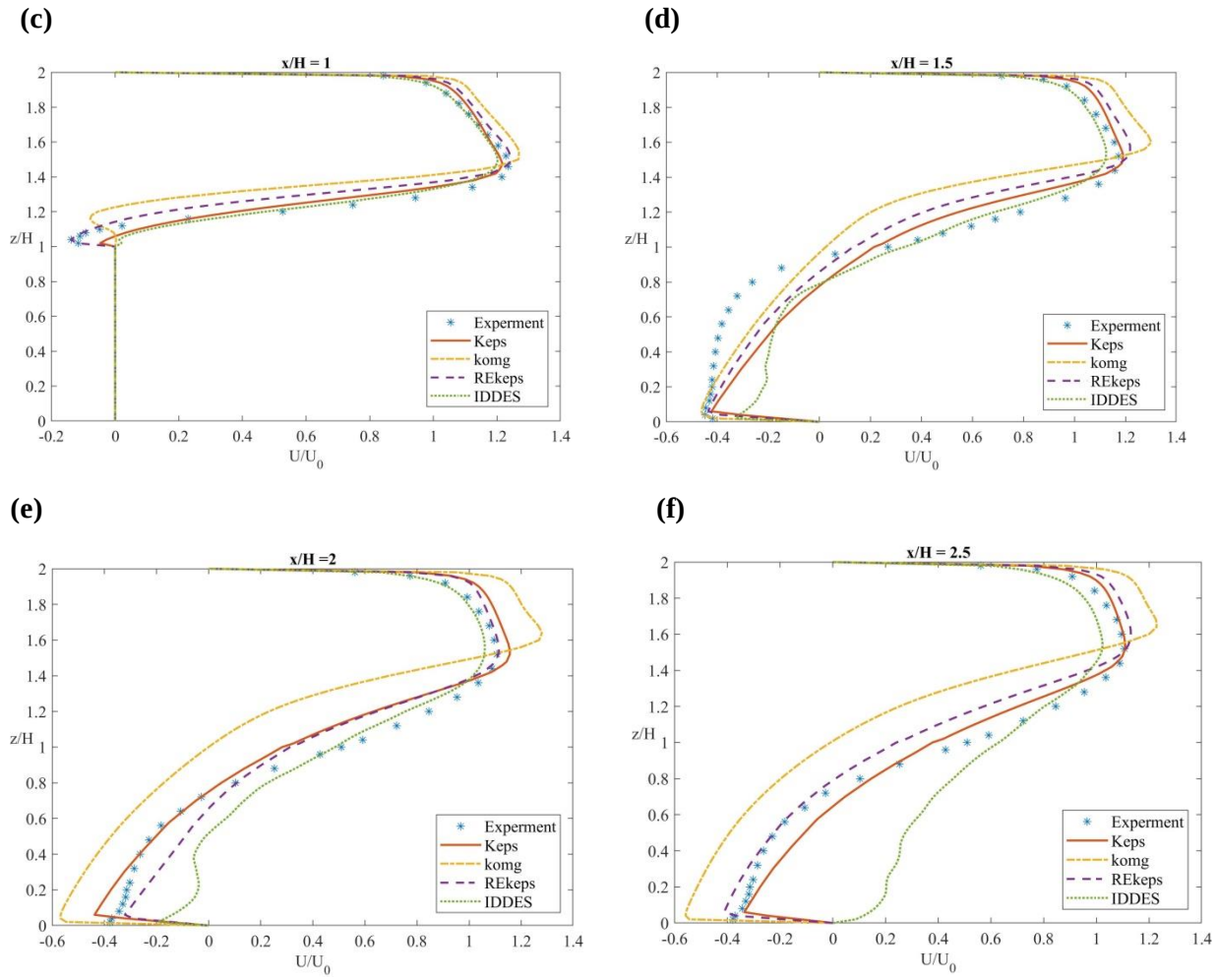

Figure 3. Comparison between the mean streamwise velocity profile computed with different turbulence model, and experimental data by Martinuzzi and Tropea (1993); (a) *x/H* = -1, (b) *x/H* = 0.5, (c) *x/H* = 1, (d) *x/H* = 1.5, (e) *x/H* = 2, (f) *x/H* = 2.5.

From Fig. 3(a), *x/H* = -1, it can be seen that the turbulence model selected has minimal significance in the velocity profile computation for the unperturbed flow. At *x/H* = 0.5, on the top of cube (Fig. 3(b)), the SA-IDDES is the case with the best agreement with the experimental results in predicting the reverse flow; all the RANS models predict a separation region at the top of the cube more thin. Whereas, at *x/H* = 1, on the downstream cube edge, in Fig. 3(c), is the Realizable k-epsilon the model that produce better agreement on the reverse flow with the experimental data. Fig. 3(d)-(f) show the mean streamwise velocity profile downwind of the cube where the recirculation region occurs and leading to reattachment; the flow recovers from separation at the front face and on top of the cube due to an adverse pressure gradient introduced by the cube in the flow path. The standard k-epsilon and the Realizable k-epsilon model produce the better results in predicting the flow recover, while the k-omega SST have the tendency to underpredict the flow

recovery, respect to SA-IDDES model that seems to overpredict the flow recovery. Similar results were obtained by Lakehal and Rodi (1997) using various versions of the k-epsilon model.

3.2 Pressure coefficient

The surface pressure coefficient, shown in Fig. 4 and defined as $C_p = (P\text{-}P_{atm})/0.5\rho U^2$, is first evaluated upstream of the cube. The position of the local pressure coefficient minimum corresponds approximately to the location of the center of the horse shoe vortex, while the location of the pressure coefficient maximum corresponds to that of the local stagnation point which causes the local increase of the surface pressure.

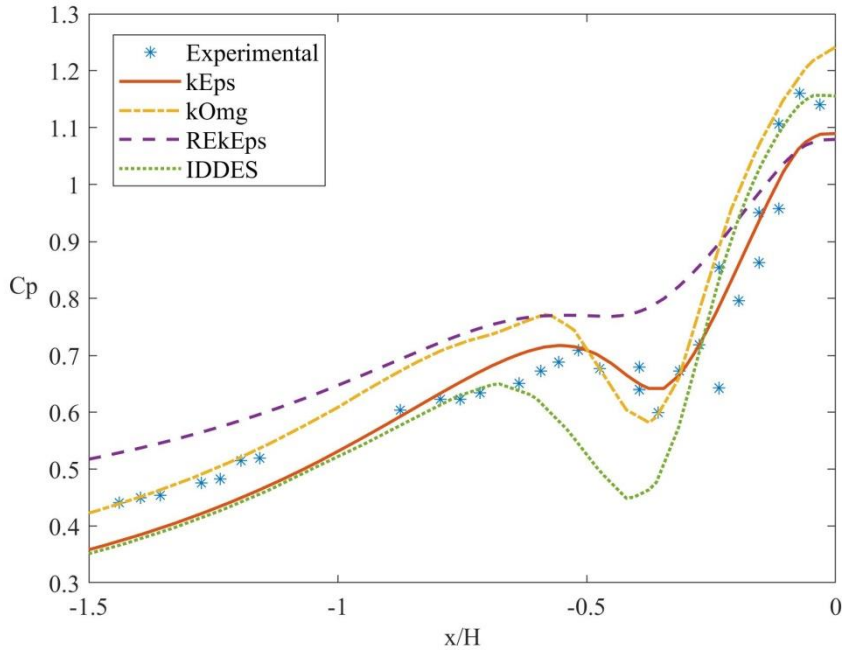

Figure 4. Comparison of C_p versus x/H along $y/H = 0$, between experiment by Martinuzzi and Tropea (1993) and numerical experiments.

It can be seen from Fig. 4, that all the models used have different areas of agreement with the experimental C_p upwind of the cube; up to a distance of $x/H = -1$ is the k-omega SST the model that produce the better agreement. Whereas, where the local minimum of pressure occurs, the Realizable k-epsilon model has the tendency in overpredict the pressure coefficient; on the other hand, the SA-IDDES model produces an underprediction of C_p. In this case are the k-epsilon and the k-omega-SST models that produce the better agreement with experimental data in predicting the local minimum of C_p. Whereas, only the SA-IDDES model is able to computing, with a good agreement, the local pressure maximum at $x/H = 0$.

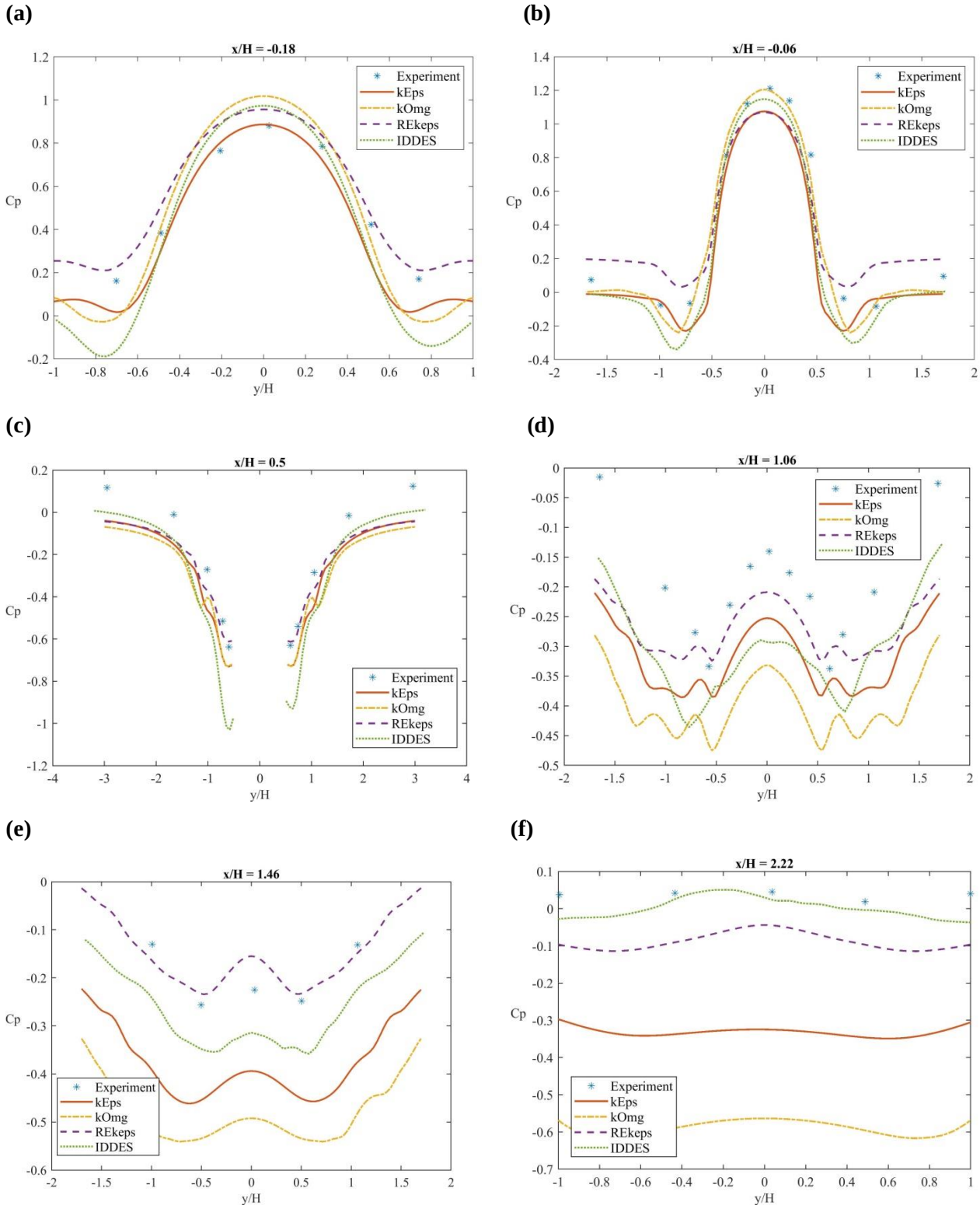

Figure 5. Comparison of C_p versus *y/H* for the flow around the cube, between experiment by Martinuzzi and Tropea (1993) and numerical experiments, (a) *x/H* = -0.18, (b) *x/H* = -0.06, (c) *x/H* = 0.5, (d) *x/H* = 1.06, (e) x/H = 1.46, (f) *x/H* = 2.22.

In Fig. 5 is reported the measured pressure coefficient in spanwise direction from the experiment of Martinuzzi and Tropea (1993), and the computed pressure coefficient from numerical

experiments at different locations *x/H*, indicating the horse shoe vortex on the side of the obstacle and the influence of the corner vortices in the recirculating region. As it can be seen from Fig. 5(a), at *x/H* = -0.18, the k-epsilon model, around *y/H* = 0, produce the best agreement with experimental data, while the k-omega SST, the SA-IDDES and the Realizable k-epsilon models produce an overestimation at *y/H* = 0, and an underestimation of C_p at the external sides, except the Realizable k-epsilon that produce the better estimation. At *x/H* = -0.06, Fig. 5(b), where the pressure local minimum occur the k-omega SST produce the best estimation of C_p around *y/H*= 0, but an underprediction is computed at *y/H* = 1 and *y/H* = -1; this underprediction is more pronounced with the SA-IDDES model. The k-epsilon model has a poor agreement with the experiment, while the Realizable k-epsilon model produce an overprediction on the external sides, and an under prediction in *y/H* = 0. In Fig. 5(c), at *x/H* = 0.5, which location is on the half edge on the cube, all the models produce an underprediction of C_p especially in the region far from the sides of the obstacle, except the Realizable k-epsilon that produce the best result. From Fig. 5(d)-(f), it can be seen that the k-epsilon and the k-omega SST models are not able to predict the C_p, resulting in a strong underestimation of the pressure coefficient, respect to the Realizable k-epsilon that presents the best agreement with experimental data beyond the obstacle. In general, those results indicate a greater wake region than the experiment. Only the SA-IDDES model has a poor agreement with the experiment at *x/H* = 2.22.

4. Summary and conclusion

Numerical experiments have been performed with the open source CFD tool OpenFoam® 1.9x, for a flow around surface mounted obstacle, with the aim of validating a turbulence model, making comparison with experimental data provided by Marinuzzi and Tropea (1993). The numerical set-up and the computation domain have been set in order to have an exact reproduction of the experiment. Comparisons of the mean streamwise velocity computed with different turbulence models, at different location upwind and downwind of the cube, have been presented. Comparisons also, have been made between the pressure coefficients computed from numerical experiments and those from the experiment upwind of the cube, and at different location upwind and downwind of the cube in spanwise direction.

In general, steady RANS turbulence models are not capable to reproduce exactly the solutions of complex flow structures, but they do provide CFD results of acceptable agreement to experimental observations. It must be emphasized that the accuracy of the solution is dependent on a number of solver variables, such as mesh configuration, numerical schemes, convergence criteria, under-relaxation factors and turbulence models employed. The results reported in this work, that are

substantially in agreement with those reported in literature (Ariff et al., 2009, Lakehal and Rodi, 1997, Krajnovic and Davidson, 2002), are obtained after benchmarking done for different configurations related to numerical schemes and meshing, looking for the best compromise between computational cost and accuracy of the solution.

It is observed that in general, the standard k-epsilon model and the Realizable k-epsilon model are able to computing mean velocity profile with a good agreement with experimental data both upwind and downwind of the cube, while the k-omega SST and SA-IDDES models, especially downwind of the cube where the recirculating region occur, produce not good results. As for the pressure coefficient, all the investigated turbulence models produce an agreement upwind of the cube with experimental observations; on the other hand, all the used models are not able to reproduce the pressure coefficient, for all the downwind of the cube distance investigated, producing a general underestimation of C_p, indicating the presence of a wake larger than the experiment, except the Realizable k-epsilon with results more close to the experiment. However, it can be noted that, different flow regions have different "best" models for their flow prediction.

Finally, the uncertainty of the solutions can depend beyond that from the choice of numerical schemes and mesh configuration, also from the experimental observations provided from Martinuzzi and Tropea (1993); the experimental data refer to time-averaged observations but the authors don't specify the average time; in addition the instrumental and experimenter uncertainty could be another possible cause of disagreement between data from numerical simulations and experiment; the last cause of disagreement can be attributed to Re_h, because in Martinuzzi and Tropea experiment the Re_h ranging from 80000 and 115000, while in the present work and in those present in literature the Re_h is fixed to $O(10^4)$.

References

Ariff M., Salim S. M. and Cheah S. C. - *Wall y+ Approach for Dealing with Turbulent Flows over a Surface Mounted Cube: Part 2 - High Reynolds Number*. Seventh International Conference on CFD in the Minerals and Process Industries CSIRO, Melbourne, Australia 9-11 December 2009.

Becker S., Lienhart H., Durst F. - *Flow around three-dimensional obstacles in boundary layers*. Journal of Wind Engineering and Industrial Aerodynamics 90 (2002), pp 265–279.

Castro I: P., Robins A. G. - *The flow around a surface-mounted cube in uniform and turbulent streams*. Journal of Fluid Mechanics, 79 (1977), part 2, pp. 307-335.

Gao Y. and Chow W. k. - *Numerical studies on air flow around a cube.* Journal of Wind Engineeringand Industrial Aerodynamics, 93 (2005), pp 115–135.

Hunt, J. C. R., Abell, C. J., Peterka, J. A., and Woo, H. - *Kinematical Studies of the Flows Around Free or Surface- Mounted Obstacles, Applying Topology to Flow Visualization*. Journal of Fluid Mechanics, 86 (1978), pp. 179-200.

Hussein H. J. and Martinuzzi R. - *Energy balance for turbulent flow around a surface mounted cube placed in a channel.* Physics of Fluids, 8 (1996), 764.

Krajnovic S. and Davidson L. - Large-Eddy Simulation of the Flow Around a Bluff Body. AIAA Journal, 40.5 (2002), pp 927-36. Web.

Lakehal D. and Rodi W. - *Calculation of the flow past a surface-mounted cube with two-layer turbulence models*. Journal of Wind Engineering and Industrial Aerodynamics, 67 & 68 (1997), pp 65-78.

Larousse A., Martinuzzi R., Tropea C. - *Flow Around Surface-Mounted, Three-Dimensional Obstacles.* Turbulent Shear Flows, 8 (1993,), pp 127-139.

Lindmeier I., Heschl C., Clauss G. and Heck U. - *Prediction of the flow around 3D obstacles using open source CFD-Software*. The Fifth International Symposium on Computational Wind Engineering (CWE2010) Chapel Hill, North Carolina, USA May 23-27, 2010.

Martinuzzi R. and Tropea C. - *The Flow around Surface Mounted Prismatic Obstacles Placed in a Fully Developed Channel Flow*. Journal of Fluid Engeneering, 115 (8) (1993), pp 85-91.

Schofield W. H. and Logan E. - *Turbulent Shear Flow Over Surface Mounted Obstacles.* Journal of Fluids Engineering, 112(4) (1990), pp 376-385.

Yang K. S. and Ferzieger J. H. - *Large-eddy simulation of turbulent flow in a channel with a surface-mounted two-dimensional obstacle using a dynamic subgrid-scale model*. 31st Aerospace Sciences Meeting, January 11-14, 1993/Reno, NV.